Imaging pathological activities of human brain tissue in organotypic culture

Caroline Le Duigou, Etienne Savary, Mélanie Morin-Brureau, Daniel Gomez-Dominguez, André Sobczyk, Farah Chali, Giampaolo Milior, Larissa Kraus, Jochen C Meier, Dimitri M Kullmann, et al.

Published in final edited form as:
J Neurosci Methods. 2018 March 15; 298: 33–44. doi:10.1016/j.jneumeth.2018.02.001.

Imaging pathological activities of human brain tissue in organotypic culture

Caroline Le Duigou[1], **Etienne Savary**[1], **Mélanie Morin-Brureau**[1], **Daniel Gomez-Dominguez**[2], **Giampaolo Milior**[1], **Farah Chali**[1], **André Sobczyk**[1], **Emmanuel Eugène**[3], **Larissa Kraus**[4,5], **Jochen C. Meier**[4], **Dimitri M. Kullmann**[6], **Bertrand Mathon**[7], **Liset Menendez de la Prida**[2], **Georg Dorfmuller**[8], **Johan Pallud**[9], **Stéphane Clemenceau**[7], and **Richard Miles**[1]

[1]Inserm U1127, CNRS UMR7225, UPMC Univ Paris 6, Institut du Cerveau et de la Moelle épinière, Paris 75013, France

[2]Instituto Cajal, Consejo Superior de Investigaciones Científicas (CSIC), Madrid E-28002, Spain

[3]Inserm U839, UPMC Univ Paris6, Institut du Fer-à-Moulin, Paris 75005, France

[4]Cell Physiology, Technische Universität Braunschweig, Braunschweig, Germany

[5]Dept Neurology Universitätsmedizin, Inst of Health, Berlin, Germany

[6]Institute of Neurology Queens Square, University College London, UK

[7]AP-HP, GH Pitie-Salpêtrière-Charles Foix, Neuro-chirurgie, Paris 75013, France

[8]Neurochirurgie, Fondation Ophtalmologique Rothschild, 75019 Paris, France

[9]Department de Neurochirurgie, Hôpital Sainte-Anne, Paris Descartes University, IMA-BRAIN, Inserm, U894 Centre de Psychiatrie et Neurosciences Paris 75014, France

Abstract

Background—Insights into human brain diseases may emerge from tissue obtained after operations on patients. However techniques requiring transduction of transgenes carried by viral vectors cannot be applied to acute human tissue.

New Method—We show that organotypic culture techniques can be used to maintain tissue from patients with three different neurological syndromes for several weeks in vitro. Optimized viral vector techniques and promoters for transgene expression are described.

Results—Region-specific differences in neuronal form, firing pattern and organization as well as pathological activities were maintained over 40-50 days in culture. Both adeno-associated virus

Correspondance: R. Miles richard.miles@upmc.fr; C. Le Duigou caroline.leduigou@icm-institute.org; E. Savary etienne.savary@gmail.com.

Contributions

CLD, ES, MMB and RM designed experiments. ES, MMB, CLD, FC, GM and EE prepared and maintained cultures. AS, DK and JCM prepared or donated viral vector constructs. CLD, ES, MMB, LK DG, LMP and RM acquired, analyzed and interpreted data. BM, JP and SC provided clinical data and performed surgery. CLD, ES and RM wrote a first version of the ms and all authors revised it.

Competing interests.

There are no competing interests to declare.

Europe PMC Funders Author Manuscripts

and lentivirus based vectors were persistently expressed from ~10 days after application, providing 30-40 days to exploit genetically expressed constructs. Different promoters, including hSyn, e/hSyn, CMV and CaMKII, provided cell-type specific transgene expression. The Ca probe GCaMP let us explore epileptogenic synchrony and a FRET-based probe was used to follow activity of the kinase mTORC1.

Comparison with existing methods—The use of a defined culture medium, with low concentrations of amino acids and no growth factors, permitted organotypic culture of tissue from humans aged 3-62 years. Epileptic activity was maintained and excitability changed relatively little until ~6 weeks in culture.

Conclusions—Characteristic morphology and region-specific neuronal activities are maintained in organotypic culture of tissue from patients diagnosed with mesial temporal lobe epilepsy, cortical dysplasia and cortical glioblastoma. Viral vector techniques permit expression of probes for long-term measurements of multi-cellular activity and intra-cellular signaling.

Graphical abstract—Organotypic cultures prepared from tissue of patients with neurological syndromes survived for 6-8 weeks in culture. A, tissue damage was limited to the first days after culture preparation, according to lactate dehydrogenase secretion. Inset shows a tissue block, culture insert and an organotypic slice after several weeks in vitro. B, viral vector application during culture application induced transgene expression after 7-10 DIV (green transgene, red NeuN). C, expression of the Ca^{2+} sensor GCaMP (green) at 20 DIV in neurons of the dentate gyrus and hilus from a temporal lobe culture. D, correlation between Ca-transients (red high, blue low) in several 10s of identified cells during synchronous activity induced by firing of a single CA3 cell in a temporal lobe culture.

Keywords

Organotypic culture; human; neurology; Viral vector; GCaMP; mTOR

1 Introduction

One goal of neuroscience research is to improve understanding of, and therapies for, human brain diseases. Animal models of pathologies have facilitated work on mechanisms and on potential drug targets. However work on human tissue (Schwartzkroin & Knowles, 1984; Cohen et al, 2002) may provide distinct insights to those from animal models (Duyckaerts, Potier & Delatour, 2008; Vargas-Caballero et al, 2016).

Surgical removal of brain tissue is an effective therapy for some pathologies including epileptic syndromes and brain tumors. Such tissue has been used for physiology (Schwartzkroin & Knowles, 1984; Köhling et al, 1998), anatomy (Maglóczky et al. 1997; Marco et al, 1997) and transcriptomic analysis (Ozbas-Gerçeker et al. 2006; Pernhorst et al, 2013). Studies on human tissue have identified novel pathological mechanisms (Köhling et al, 1998; Cohen et al. 2002; Pallud et al. 2012).

But, powerful recent techniques cannot be applied to acute brain tissue (Jones et al, 2015). Several days are needed to express transgenes delivered by viral vectors. With selective promoters, specific cell types may be targeted (Tye et al, 2011). This approach has driven

progress in work, including optical recording and stimulation (Emiliani et al, 2015), where probes or other molecules (Paquet et al, 2016) must be expressed in brain cells.

Stable culture techniques (Gähwiler et al, 1997) for human tissue could resolve this difficulty. Brain tissue from epileptic patients may be kept in organotypic culture (Eugène et al, 2014). Here we generalize techniques to tissue diagnosed with three neurological syndromes. We assess the stability of neuronal physiology, organization and pathological activity in culture. Techniques for transduction of transgenes carried by viral vectors are optimized for adeno-associated- (AAV) and lentiviral (LV) vector constructions. Transgenes transduced included the Ca^{2+} sensor GCaMP (Chen et al. 2013) and a FRET-based reporter of mTORC1 kinase activity (Zhou et al, 2015). Such probes enable long-term optical interrogation of multi-cellular activity and intra-cellular signaling in an epileptic human brain.

2 Materials and Methods

2.1 Temporal lobe tissue from epilepsy patients

Slices for organotypic culture were prepared from surgically excised tissue blocks of human temporal lobe and peri-tumoral or dysplasic cortex. Tissue was obtained from: (a) adult patients diagnosed with pharmaco-resistant mesial temporal lobe epilepsy (MTLE) associated with hippocampal sclerosis (n=20; Neurochirurgie, Pitié-Salpêtrière). The type of hippocampal sclerosis (HS) according to ILEA classification (Blümcke et al, 2013) is indicated; (b) adult patients diagnosed with diffuse low-grade gliomas (Glioma, n=3; Neurochirurgie, Sainte Anne); and (c) adult patients diagnosed with focal epilepsies associated with cortical dysplasia (Dysplasia, n=3; Neurochirurgie Clinique Rothschild). Sparing use of cauterization during surgery provided a higher quality of organotypic slices, judged by culture survival and the ease of recording from neurons. All patients gave their written, informed consent. Protocols were approved by the Comité de protection des personnes, Ile de France 1 (C16-16, 20152482) and the Consultatif National d'Ethique. The gender, age and diagnosis of patients who donated tissue for the study is given in Supplementary Table 1.

2.2 Preparation of organotypic cultures

Tissue blocks were transported in a solution containing: NaCl, 87; $NaHCO_3$, 26; NaH_2PO_4, 1.2; KCl, 2.5; $CaCl_2$, 0.5; $MgCl_2$, 10; sucrose, 75 and d-glucose, 25 (mM), at 2-10 °C, gassed with 95% O_2/5% CO_2, of pH 7.3 and osmolarity 305-315 mOsm. Connective tissue and blood vessels were cleaned before cutting 300 μm thick slices with a vibrating microtome (HM650V, Microm) in the same solution and in sterile conditions under a flow hood (Supplementary protocol for further detail).

After cutting, slices were washed for 15 min in Hanks balanced salt solution with added HEPES (20 mM; room temperature, gassed with 95% O_2/5% CO_2, pH 7.3, osmolarity 305-315 mOsm). They were then placed on membranes of an insert in a 6-well plate (30 mm Transwell, Merck-Millipore). 1 ml of culture medium was placed in each well. The defined medium (Eugene et al, 2014) was made by adding components (Supplementary Protocol,

Table 4) to a mixture of BME, DMEM-F12 and N2 media (Invitrogen). When the 6-well culture plates were transferred to an incubator, slices were maintained at an interface between the medium and a 5% CO_2 in air atmosphere at 37°C as in Stoppini et al (1991).

The medium was changed every 1 or 2 days and for the first week contained penicillin (100 U/ml), streptomycin (0.1 mg/ml) and amphotericin B (0.25 μg/ml). Cell damage was estimated by measuring lactate dehydrogenase (LDH; Koh & Choi, 1987) levels in the medium. Cultures were transduced with viral vector constructions (Supplementary protocol, Supplementary Table 2) either during culture preparation or after 7 days in culture.

2.3 Electrophysiological recordings

Recordings from organotypic slices were made in a chamber mounted on an upright microscope (BX50WI, Olympus). They were perfused at 3 $ml.min^{-1}$ with a solution containing NaCl 119, KCl 2.5, $NaHCO_3$ 26, NaH_2PO_4 1, $MgCl_2$ 1.3, $CaCl_2$ 2.5 and glucose 15 (in mM), equilibrated with 5% CO_2 in 95% O_2 (pH 7.3, 297 mOsm). Temperature was controlled at 32–35ºC. We attempted to induce ictal-like activity by increasing neuronal excitability with a solution containing NaCl 119, KCl 10, $NaHCO_3$ 26, NaH_2PO_4 1, $MgCl_2$ 0.1, $CaCl_2$ 2.5 and glucose 15 (in mM). In some experiments, neuronal excitability was reduced by increasing divalent cations, $CaCl_2$ and $MgCl_2$, or decreasing KCl.

Neurons were visualized with infra-red differential interference contrast microscopy. Current clamp records were made in whole cell mode with pipettes of resistance 4–5 mΩ, containing K gluconate 117.5, KCl 17.5, HEPES 10, EGTA 0.2, NaCl 8, MgATP 2, Na_3GTP 0.3 mM (pH 7.2, 290-300 mOsm). Signals were amplified with a Multiclamp 700B amplifier (Molecular Devices), filtered at 5 kHz, digitized at 10 kHz, and recorded with pClamp (Molecular Devices) running on a PC. Neuronal input resistance, R_{in}, was calculated from voltage deflections of less than 20mV, induced by step current injections of duration 1 s. Rheobase was defined as the minimal current which elicited an action potential during a step depolarizing current. Firing pattern and frequency were measured in responses to depolarizing steps of 400 pS and duration 1 sec. Records were accepted when R_{in} was greater than 50 mΩ, resting membrane potential more negative than -55mV and depolarizing current steps evoked multiple, overshooting action potentials. The anatomy of recorded cells was revealed post-hoc in some experiments by including biocytin (4 mg/ml) in the recording pipette. Extracellular recordings were made with glass pipettes of resistance 0.5-1 MΩ, filled with bath solution and bandpass-filtered from 1-5000 Hz. Focal stimulation with bipolar stainless steel electrodes was used to induce synaptic events and epileptiform activities.

2.4 Imaging, probes and data acquisition

Fluorescent images were captured at the same time as electrophysiological recordings, with a spinning disk confocal system (CSU-X1, Yokagawa). Objectives included a 20×, 1.0NA and a 4x, 0.28 NA (water immersion, Olympus). Fluorophores were excited by lasers of power 100mW, emitting at 405 (violet), 491 (green), 561 (yellow) and 642 nm (red). Laser light was coupled to the system with a quad-band dichroic mirror (405/488/568/647 nm; Semrock).

For calcium imaging, GCaMP6 (Chen et al, 2013) was excited at 491 nm. Emitted light was filtered with a GFP/mCherry double 488/568 bandpass filter (Semrock) mounted between the spinning disk unit and an EMCCD camera (512x512 pixels, 16μm; Photometrics). Emitted signals were acquired at frame rates of 5-30 Hz with Metamorph software (Molecular Devices) and analyzed with Metamorph, ImageJ or with Matlab.

Changes in cellular mTORC1 activity were studied by fluorescence resonance energy transfer (FRET) in a construction consisting of a kinase activity-dependent linker expressed between a cyan FP and a yellow FP FRET pair (TORCAR; Zhou et al, 2015). Dual - emission ratio imaging was performed with a 445/514/593nm Yokogawa dichroic beamsplitter and two emission filters, 480DF40 (CFP) and 530DF30 (YFP channel). Images were acquired, with Metafluor software (ver6.2), from both channels every 30 s with exposure times of 50–300 ms. Fluorescence images were corrected for background by deducting signals from regions with no cells from CFP and YFP signals. Traces were normalized by setting the emission ratio during a control period before experimental manipulation.

2.5 Image analysis

Calcium dependent fluorescence signals from neurons expressing GCaMP were measured as the average of all pixels in a manually defined region of interest (ROI) around the soma. ΔF/F values were calculated as $\Delta F/F=(F_t-F_0)/(F_0-F_{bg})$ where F_t was the fluorescent signal at time t, F_0 was the mean fluorescence of 10 baseline frames and F_{bg} was the mean fluorescence of 10 baseline frames in a region with only background signal.

Correlations between Ca signals (F) in different cells were analyzed with routines written in Matlab (Mathworks v.10b). Multiple neurons were identified from the accumulated standard deviation image of Ca^{++} signals during a recording and confirmed manually. Fluorescence signals from multiple ROIs, corresponding to neuronal somata, were stored as ΔF/F values over time, interpolated to 30 Hz, after baseline subtraction. Ca^{++} signal peaks associated with interictal events were detected using a threshold of > 3 baseline SD, maintained above 0.5SD for more than 0.5 sec. The time course of during spontaneous or triggered epileptiform events was defined with respect to first spike generated by a simultaneously recorded cell.

Matrices were constructed to examine correlation between activities in different neurons. Each matrix element was the Pearson coefficient of correlation, r, between Ca^{++} signals from cell pairs during a window of 2 s starting with an epîleptiform event peak signal. R-values are high (near 1) for cell pairs with similar Ca^{++} signal dynamics, low (near 0) for pairs with a strong Ca^{++} signal in one cell but not the other, and tend to be reduced when Ca^{++} signals in different cells are weakly synchronous in time (2-3 frame differences). Cells were ordered in matrices according to the timing of Ca^{++} signal with respect to initiated epileptiform events (at 10% of the peak). In this way cells stimulated to initiate epileptiform events exhibited the shortest latency and came first in the ordering procedure.

Europe PMC Funders Author Manuscripts

2.6 Anatomy

Slices used for anatomy were fixed for 24 hrs in 4% paraformaldehyde in phosphate buffered saline (PBS, pH 7.3) at 4 °C and stored in 0.4% Na-azide in PBS. They were transferred to a 30% sucrose in PBS overnight and exposed to 3 freeze-thaw cycles. In some experiments, biocytin-filled neurons were revealed with streptavidin conjugated to Alexa 647 (Invitrogen). A blocking step before the streptavidin-biotin reaction, used exposure for 2 hrs to 10% normal donkey serum, 0.5% Triton X-100, with 2% milk powder. Slices were incubated for 48h at 4°C with streptavidin-Alexa to reveal biocytin. In other work, antibodies used for immunostaining. Incubation with a primary antibody was made for 48h at 4°C, and after PBS washing, incubation overnight at 4°C with a secondary antibody. Primary antibodies were used against: GFP (Life technologies A11122, polyclonal, rabbit, dilution 1:500), NeuN (Millipore MAB377, monoclonal, mouse, dilution 1:250), and GFAP (Millipore ab5541, polyclonal, chicken, dilution 1:500). Secondary antibodies were conjugated with Alexa Fluor 555 or 488 (dilution 1:500; Invitrogen). Sections were counterstained with the nuclear stain DAPI (10 μg/mL, 15 min) and mounted on glass slides with ProLong® Gold Antifade Reagent (Life Technologies).

Neurons and transducted cells were counted with an automated fluorescent microscopy system (Arrayscan with HCStudio software, Thermo-Fisher). Transfected cells were identified using an anti-GFP antibody which recognizes the GCaMP probe (Chen et al, 2013). Neurons were identified with and anti-NeuN antibody. Excitation/emission filter sets (XF93, Omega Optical) were used to visualize fluorescent signals corresponding to GFP (excitation 549/15 nm), NeuN (650/15 nm) and DAPI (386/25 nm). Images were acquired with a cooled 12-bit charge-coupled camera (2208x2208 pixels of 4.54μm, Photometrics X1, N01X1SHTLAS). Optical stacks were acquired over z-distances of 50-100 μm at interval 10 μm, in middle regions of the dentate gyrus of organotypic slices. GFP+ and NeuN+ cells were detected with an intensity threshold to identify objects colocalized with a DAPI nuclear signal. After identification, cells were accepted or rejected visually from on shape and size criteria.

Confocal images were made with a microscope (Leica SP2 AOBS, AOTF) using laser excitation wavelengths of 405, 488 and 543 nm and a 40x objective of NA 1.25. Images were acquired at a 2048 x 2048 resolution for a final voxel size of 0.18 μm in x and y and 1.25 μm in z.

3 Results

3.1 Survival of organotypic cultures of adult human tissue

Brain tissue was obtained after operations on patients aged 3-62 years (Supplementary Table 1), diagnosed with temporal lobe epilepsy (n=24), low-grade cortical glioma (n=3) or cortical dysplasia (n=3). Organotypic cultures prepared from this tissue (Supplementary Protocol) were maintained for up to 60 days. Lactate dehydrogenase (LDH) levels in culture medium, an index of cell damage (Koh & Choi, 1987), were high over the first 2-3 days in vitro (DIV) and then fell to low levels (Fig. 1A). Terminating antibiotic treatment at 7DIV transiently increased LDH levels, but viral vector application (at 0 or 7DIV) did not.

Neurons were recorded from all brain regions in acute tissue and in cultures up to 60DIV. Fig. 1B shows the success rate to obtain acceptable whole-cell records as a proportion of attempts. Recorded neurons were accepted with a resting potential more negative than -55 mV and multiple action potentials induced by current injection. Cells not meeting these criteria typically generated only a single action potential from more hyperpolarized resting potentials.

The stability of neuronal physiology with time in culture was assessed from dentate granule cells (Fig. 1C). The frequency of firing induced by current injection (400 pA, 1s) in acute slices was 19 ± 2 Hz (mean ± sem, n=20). At 14 DIV, it was 18 ± 2 Hz (n=10) and at 40-50 DIV granule cells were more excitable, with firing frequency 30 ± 2 Hz ($p < 0.001$, t-test, n=35). Neither rheobase nor resting potential changed significantly. Resting potential was 71 ± 2 mV at 0DIV (n=20), -and 69 ± 2 mV at 50 DIV (n=17; p=0.31, t-test). Possibly an increased input resistance as cultures age (Fig. 1C) underlies the increased firing. At 40-50 DIV, dendritic swelling was apparent for some neurons (not shown).

3.2 Maintenance of regional differences in neuronal organization, form and physiology

Are region-specific features of neuronal physiology and morphology (Fig. 2) maintained in culture? We assessed regional organization from Golgi-like images of neurons virally transduced with the Ca-probe GCaMP (Supplementary Table 2) and labelled with an anti-GFP antibody (Chen et al, 2013). Physiology and morphology were assessed from records with biocytin-containing electrodes.

Immunostaining of GCaMP-transduced dentate cells at 14-40 DIV revealed a loosely packed layer of neuronal somata with profuse apical dendrites (Fig. 2A). Dentate granule cells were typically silent, but fired regularly with adaptation in response to injected current (n=51). Their resting membrane potential was -69 ± 1 mV and input resistance was 98 ± 8 mΩ (n=51; Supplementary Table 3). Depolarizing synaptic events were detected in most records. Biocytin-filled cells possessed round somata of diameter ~15 μm and profuse apical dendrites. Insets show sections of dendrite and axon.

CA2/3 pyramidal cells were organized in a somatic layer with aligned apical and basal dendrites (Fig. 2B). Some CA2/3 neurons fired regularly (15/26) in response to injected current (400 pA, 1s), others discharged bursts of action potentials (11/26). Resting potential was -68 ± 1 mV and R_{in} was 83 ± 8 mΩ (n=26; Supplementary Table 3). Biocytin-filled CA2/3 pyramidal cells possessed multiple basal dendrites and a thick proximal apical dendrite.

In the CA1 region, few GFP+ elements were detected. Whole-cell records were usually unsuccessful. This is consistent with a limited or absent neuronal migration in culture, together with the pre-surgical neuronal loss in this brain area of patients with temporal lobe epilepsy.

Subicular cell somata were loosely packed with aligned apical and basil dendrites (Fig. 2C). Stimulated by current injection, some subicular cells fired in bursts of action potentials (5/9), while others discharged regularly (4/9). Resting potential was -75 ± 6 mV and R_{in} was 54

± 10 mΩ (n=9; Supplementary Table 3). Biocytin-filled, subicular pyramidal cells possessed a thick proximal apical dendrite and multiple basal dendrites.

Cortical pyramidal cell somata were loosely distributed and apical dendrites were aligned (Fig. 2D). Superficial, layer II-III, cells fired repetitively with moderate adaptation in response to current injection. Resting potential was -65 ± 2 mV and R_{in} was 106 ± 13 mΩ (n=23; Supplementary Table 3). Biocytin-filled pyramidal cells possessed large somata, a thick proximal apical dendrite and multiple basal dendrites.

Overall, these data show that regional organization, neuronal physiology and morphology at 14-40 DIV are comparable with observations from work on acute slices of human dentate gyrus (Selke et al. 2006), CA2/3 (Wittner et al, 2009), subiculum (Huberfeld et al, 2007) and dysplasic (Cepeda et al, 2014) or peritumoral cortex (Pallud et al, 2014).

3.3 Optimization of viral vector transduction

Supplementary Table 2 lists viral vectors used. Transduction procedures were optimized with AAV9-hSyn-GCaMP6f using the dentate gyrus as a test region (Fig. 3). The transgene GCaMP6 was detected by immuno-staining against GFP. An antibody against NeuN was used to assess target specificity and neuronal survival in culture. We compared viral vector application at ODIV, during culture preparation, and at 7DIV (Mioduszewska et al 2008)

At 7 days after vector application at 0 DIV, the mean proportion of $NeuN^+$ neurons that were also GFP^+ was 31.8 ± 1.5% (n=96 counts from fields of 1.2 x 1.2 x 0.05 mm in 3 slices). When vectors were applied at 7 DIV, the transduction rate was 27.0 ± 2.6% (n=96 fields in 3 slices; p= 0.15). Mean transduction levels were 26-35% over 7-28 days after vector application at 0 or 7 DIV (Fig. 3A).

Neuronal survival was estimated by comparing the density of $NeuN^+$ cells in culture with that in freshly-cut slices (Fig. 3B-D). In acute slices, cell density was 34.2 ± 1.8 cells/$100\mu m^3$ (n= 24 counts, 3 slices). At 13-15 DIV there were 30.0 ± 1.8 $NeuN^+$ cells/$100\mu m^3$ (n=12, 5 slices). The survival rate estimate ~88%, is uncorrected for potential flattening in culture. Values of 78-95% were estimated for other time points. Survival did not differ if vectors were applied at 0 or 7 DIV (p= 0.26; Fig. 3B).

In further work, vectors were applied during culture preparation (0 DIV), since neither transgene expression nor neuronal survival differed greatly when they were applied at 0 or 7 DIV. Expression occurred reliably by 10-14 DIV. Records of transduced cultures were made from 14-40 DIV to reduce effects of enhanced neuronal excitability in aged cultures (Fig. 1C).

We also explored the specificity of different vector and promoter combinations in organotypic cultures (Supplementary Table 3). Transduction with lentiviral (LV) vectors was similar to that with AAV vectors. Transgene expression was first detected at 5-6 days and was stable after 10-14 days. (Supplementary Fig. 1A-D). Different cell-specific transduction patterns could be achieved. The CMV promoter with an LV vector induced expression in GFAP+ astrocytes as well as neurons (Supplementary Fig. 1A, B) while expression was selectively neuronal when the hSyn promoter was coupled with LV vectors (Supplementary

Fig. 1C-D). Selective transduction in a specific neuronal subset was achieved using the CaMKII promoter with AAV5 vectors (Supplementary Fig. 1E). The CMV promoter with AAV9 induced largely neuronal expression (Supplementary Fig. 1F), possibly due to an AAV tropism.

An unexpected pattern of transgene expression occurred with LV vectors coupled to the hybrid e/hSyn promoter (Hioki et al, 2007). Expression was weak in granule or cortical neurons, but stronger in another cell population. Fig. 4A compares expression of the AAV9-hSyn vector (red) and LV-e/hSyn vector (green) in the dentate gyrus. Electrical properties of differentially transduced cells also differed (Fig. 4B). In cells expressing the LV-e/hSyn transgene, stimulation induced at most one action potential (cf Fig. 1B, unacceptable records) while multiple spikes were generated in neurons transduced by AAV9-hSyn, Input resistance was higher (225 ± 15 versus 98 ± 8 MΩ; n=20, p=0.032), in LV-e/hSyn transduced cells and after biocytin filling, clusters of 4-6 coupled neurons were revealed (Fig. 4C; n=4 of 4 fills). Multiple cells were never detected after biocytin-filling of neurons transduced with AAV9-hSyn vectors. Finally, these cells were immunopositive for reelin (Fig. 4D), suggesting they may correspond to intermediate neuronal progenitor cells or immature adult-born neurons (Hodge et al, 2008; Bonaguidi et al, 2012). The selective transduction may depend on the affinity of LV, but not AAV, for dividing cells and a negative tropism of LV with the e/hSyn promoter for adult dentate granule cells (van Hooijdonk et al, 2009).

Neurogenesis and differentiation in an epileptic brain remain controversial (Pineda & Encinas, 2016). One factor controlling the fate of progenitor neurons is the kinase mTORC1 (Paliouras et al, 2012; Venkatesh et al 2015). Taking advantage of the selective targeting of LV-e/hSyn, we used a FRET-based reporter (Zhou et al, 2015) to examine basal levels and seizure-induced changes in mTORC1 kinase activity in immature neurons. Basal FRET emission ratios in neurons of the dentate region were in the range of 0.3-1.5 (n = 35 cells; Fig. 4E). Seizure-like activity changed kinase activity signals according to their basal kinase level (n=7 cells; Fig. 4F). For cells with a basal FRET ratio less than 1, or low mTORC1 activity, seizure discharges induced a transient increase of 12 ± 3 % (n=3 cells; Fig4G) while in cells with higher resting activities, it induced a decrease of 17 ± 2 % (n=4 cells; Fig4H). Seizure activity thus acts homeostatically to maintain mTORC1 activity in immature neurons.

3.4 Maintenance of epileptiform population activities in culture

A maintained pathological activity would show that human cultures retain functional properties of in situ tissue. We explored epileptiform activities in simultaneous electrical and optical records of neuronal calcium transients (Fig. 5) from cultures transduced with GCaMP6 (Trevelyan et al, 2006).

Simultaneous, transient increases in Ca^{++} occurred without stimulation in CA2/3 neurons and those of the hilus and dentate gyrus in most cultures of sclerotic hippocampus (n=42 from 20 of 24 patients). Local field and whole cell records revealed Ca-transients corresponded to recurring interictal population discharges (duration 0.2-2 sec, frequency 0.1-1 Hz; Fig. 5A).

Prolonged ictal-like events were induced in 9 cultures from 11 patients by increasing neuronal excitability (external K^+10 mM; Mg^{2+} 0.1 mM). Typically, bursts of duration 10-20 sec occurred initially and then evolved into oscillations at ~0.3Hz. As shown in Fig. 5B, ictal-like activity was synchronous over distances of several mm.

In cultures of peritumoral cortex, synchronous Ca-transients occurred spontaneously (Fig. 5C; n=3 cultures from 2 of 4 patients). Simultaneous records from single neurons revealed interictal events of duration 0.1-0.5 sec, recurring at 0.01-0.02 Hz. Increasing excitability (K + 10, Mg2+ 0.1 mM) strengthened synchrony (n=5 cultures from 4 patients) inducing ictal-like events of duration 20-30 sec typically in most neurons but not all neurons. Ca-transients and field potentials recurred at 0.01-0.3 Hz (n=5 cultures).

Some cultures of dysplasic cortex generated spontaneous, simultaneous Ca^{2+} transients, correlated with local field potentials, in neurons within a radius of ~2mm (Fig. 5D; n=2 of 6 cultures from 3 patients). Neurons discharged 2-20 action potentials during events of duration 0.1-0.4 sec repeated at 0.1 Hz (Fig 5D). When neuronal excitability was increased (K^+, 10 and Mg^{2+}, 0.1 mM), population bursts at 0.3-1.5 Hz were detected as Ca-transients, single cell firing or extracellular fields in all dysplasic cortex cultures (n=6 from 3 patients).

In summary, epileptiform activities are maintained in organotypic culture. Temporal lobe tissue is more epileptogenic than peritumoral or dysplasic cortex. Epileptiform activities were suppressed by the AMPA receptor antagonist NBQX (10-20 μM; sclerotic hippocampus, n=5 cultures; dysplasic cortex n=3; peritumoral cortex, n=3). The NMDA antagonist APV (100 μM) reduced intensity and prolonged intervals between interictal-like and ictal-like events. We did not detect a systematic increase in epileptiform behavior with time. Synchronous activity was detected in 53 % (18/34) of slices at 12-20DIV and increased to 66% (10/15) at 30-40DIV but the frequency decreased from 3.2 ± 0.1 Hz at 12-20DIV to 0.5 ± 0.02 at 30-40DIV.

3.5 Single cell stimulation and Ca-imaging to probe the functional anatomy of epileptic circuits

Some single pyramidal cells in acute rodent slices can influence or trigger epileptiform activity (Prida et al. 2006). To visualize the synaptic circuits involved, we combined single cell stimulation in temporal lobe cultures with data on Ca-transients induced in GCaMP-transduced neurons (Kwan & Dan, 2012). We found firing in 8 of 37 CA2/3 pyramidal cells and in 5 of 51 granule cells triggered widespread Ca-transients in temporal lobe cultures (Fig. 6A-C). Epileptiform field potentials were initiated within 20-100 ms of trigger cell firing. Numbers of active neurons in the CA2/3 region, the hilus and the dentate gyrus was assessed from Ca-transients. During triggered events transients were detected in 81 ± 16 neurons (n=7 slices; field 1.6x1.6 mm) compared to 60 ± 11 cells during spontaneously generated events (n=7; p=0.309).

Reducing neuronal excitability can discriminate between mono-synaptic and poly-synaptic circuits by suppressing firing of intercalated cells in multi-neuron chains (Nicholls & Purves, 1970). Increasing external Ca^{++} (from 2.5 to 3.5 mM; n=8) reduced cellular firing and field potential duration (Fig. 6D, E). Active neuronal ensembles were visualized with

matrix plots that correlated the amplitude of Ca-transients in all cells (Fig. 6D, E; Supplementary methods). Paired records from trigger cells and follower neurons let us define the synaptic relations between them. At control excitability, trigger cell activity induced firing in follower cells as well as a Ca-transient shown in the matrix-plot (Fig. 6F). At lower excitability, the trigger cell initiated a short-latency EPSP (3.2 ± 0.1 ms) and a Ca-transient, evident in the matrix plot (Fig. 6F). In contrast for the pair of Fig. 6G, lowering excitability revealed a poly-synaptic IPSP (latency 14.0 ± 1.0 ms) and no Ca transient (Fig. G).

These data show that trigger cells initiate firing in a larger neuronal population via both mono- and poly-synaptic pathways. Matrix representations in control and reduced excitability permitted separation of these populations. In 6 experiments, we compared effects of trigger cell firing in control conditions and at lowered excitability (Fig. 6H, I). Ca-transients were detected in 84.6 ± 9.8% neurons in control conditions. They were maintained in 29.6 ± 22.7 % of cells at low excitability. This approach also let us map mono- and poly-synaptic interactions for epileptiform synchrony. Fig. 6J plots the spatial distribution of presumed mono-synaptic targets, where a Ca-transient was detected in both control and low excitability (red), and presumed poly-synaptic targets (blue), with a Ca-transient observed only in control excitability.

4 Discussion

Human brain tissue may provide specific information on human neurological syndromes. This report describes the preparation and maintenance of organotypic brain cultures from patients with three different syndromes. Cultures retain region-specific neuronal physiology and morphology as well as epileptic activity over several weeks. Selective transgene expression may be achieved using viral vector constructions. Expression of the Ca indicator GCaMP (Chen et al, 2013) let us examine neuronal population activities and a FRET-based probe permitted monitoring of mTORC1 kinase activity. Thus organotypic cultures of tissue derived from operations on adult patients open new avenues for work on human neurological syndromes.

4.1 Organotypic culture: neuronal survival and maintained regional diversity

Organotypic cultures of brain slices (Gahwiler et al, 1997; Stoppini et al, 1991) have typically been prepared from tissue of young animals. Here we used brain tissue of patients aged from 3 to 62 years. We noted no major difference in culture survival or preparation for tissue from the two youngest patients, 3 and 4 years. A defined medium adapted for adult tissue (Supplementary Table 4) contained low concentrations of amino acids, no growth factors, reinforced anti-oxidant activity and glucose, lactate and pyruvate as energy sources (Eugène et al, 2014). Further changes might further optimize tumor survival and growth in cultures of peri-tumoral cortex (Seifert & Sontheimer, 2014).

Region-specific neuronal organization and properties were maintained over 5-6 weeks for the dentate, CA2/3 and the subicular regions as well as the cortex. There was no significant neuronal migration into the sclerotic CA1 region. Dentate granule cell electrophysiology in culture was initially comparable to that in acutely prepared slices (Supplementary Table 3).

Europe PMC Funders Author Manuscripts

It remained so, until 40-50 DIV (Fig. 1C) when excitability increased and local dendritic swelling was also evident. Stable neuronal physiology and maintained epileptiform population activity facilitate long-term studies on human pathologies. A conserved neuronal identity and adult synaptic connectivity may provide advantages over partially differentiated pluripotent stem cells for some questions.

4.2 Optimized expression of genetically coded probes

Viral vector mediated transgene expression enhances possible uses of human tissue in organotypic culture. Transgenes carried by AAV or LV vectors, applied during culture preparation were stably expressed at 10-14 DIV so that genetically encoded probes could be exploited over ~4 weeks.

We found LV vectors were somewhat more difficult to use than AAV vectors. Titres had to be adjusted to induce sufficiently strong transgene expression without provoking tissue swelling, presumably due to an immune response (Follenzi, Santambrogio & Annoni, 2007). Distinct promoters targeted distinct cell types largely as predicted. The exception was the e/hsyn promoter which favored transgene expression in progenitor or adult-born neurons with immature electrical properties and coupled in small groups. Exploiting this selectivity, we asked how activity of the mTORC1 kinase (Zhou et al, 2015) is changed in immature cells by seizure-like events. Human organotypic cultures will facilitate studies on how mTORC1 activity affects neurogenesis and maturation in epileptic tissue (Hattiangady & Shetty, 2010; Mahoney et al, 2016).

4.3 Single cell stimulation and Ca-imaging as a tool to map functional epileptic circuits

We found that epileptiform events could be initiated by firing in ~15% of single cells tested (Prida et al, 2006). Imaging neuronal Ca transients let us probe the synaptic circuits involved (Kwan & Dan, 2012). Results suggest epileptiform firing is initiated by mono-synaptic connections and proceeds via poly-synaptic neuronal chains, which cease transmission as excitability is reduced. Thus recurrent excitation (Le Duigou et al, 2014) synchronizes human epileptic population activity as well as exerting more subtle physiological effects (Brecht et al, 2004; Li, Poo & Dan, 2009).

Exuberant axonal growth and synaptogenesis are commonly associated with organotypic culture. However, our use of adult, human rather than immature, rodent tissue as well as an absence of growth factors in the culture medium may have limited exuberant over-connectivity. In paired records, the frequency of mono-synaptic connections was lower than values of ~50% from slice cultures of rat hippocampus (Debanne et al, 1995). Ca-imaging suggested that single cells directly excited a minority of potential post-synaptic partners (Fig. 6). Furthermore, even if neuronal excitability was increased at 40-50 DIV (Fig. 1C), epileptiform activities did not change greatly with time in culture (McBain et al, 1989; Lillis et al 2015) as might expected with a strong synaptogenesis of recurrent connections.

4.4 Perspectives

These techniques will facilitate new approaches to questions on human neurological disorders. One use is long-term, imaging-based tests of the efficacy and safety of molecules

Europe PMC Funders Author Manuscripts

to control epileptic activities (Long, Fureman & Dingledine, 2016). Peritumoral tissue cultures (Chadwick et al, 2015) will facilitate work to understand interactions between the growth and infiltration of gliomas and the aggravation of epileptic activities and to test on molecules to control them. Finally gene transfer with viral vectors is becoming a therapeutic option for brain pathologies (Lentz, Gray & Samulski, 2012). Organotypic slices would provide a suitable context to improve vectors and test promoters in human brain, to measure possible toxicity and to explore transgene function (Hoquemiller et al, 2016).

Supplementary Material

Refer to Web version on PubMed Central for supplementary material.

Acknowledgements

This work was supported by grants from the ERC (322721, RM), ERAnet (CIPRESS; ANR-12-NEUR-0002-03, RM), Investissements d'Avenir (ANR-10-IAIHU-06, ICM) and NeurATRIS (ANR-11-INBS-0011, ICM). LMP is supported by grants BFU2015-66887-R by the Spanish MInistry of Economy and by the Fundación Tatiana Perez de Guzman el Bueno. JCM is supported by grants from the DFG in Germany (SPP 1784, grant No. ME2075/7-1) and the BMBF (Era-Net NEURON II CIPRESS). DMK is funded by grants from the Wellcome Trust and the MRC. DGD is funded by a PhD fellowship by the Spanish Ministry of Economy (BES-2013-064171). We thank Jean-Christophe Poncer and P Ravassard (ICM) for helpful comments and discussions. D Akbar (ICM) helped with automated cell count analysis and K Fidelin (ICM), S Cumberland and K Toth (Laval, Quebec) with Ca signal analysis. The GENIE Program of Janelia Farm is thanked for the GCaMP6 construction and J. Zhang (Dept Phamacology, Johns Hopkins) for the TORCAR plasmid. We thank A Schönherr (NeuroCure Core, Charité, Berlin) for AAV9 particles, A Snowball (Inst Neurol, UCL, London) for AAV5 particles, C Bernert and M Semtner (MDC Berlin) for help with the mCherry reporter construct and J Johnston (Penn Vector Core, Univ. Philadelphia) for the pAdDeltaF6 (AAV9) plasmid. We have no conflict of interest.

References

Blümcke I, Thom M, Aronica E, Armstrong DD, Bartolomei F, Bernasconi A, Bernasconi N, Bien CG, Cendes F, Coras R, Cross JH, et al. International consensus classification of hippocampal sclerosis in temporal lobe epilepsy: A task force report from the ILAE commission on diagnostic methods. Epilepsia. 2013; 54:1315–1329. 2013. [PubMed: 23692496]

Bonaguidi MA, Song J, Ming GL, Song H. A unifying hypothesis on mammalian neural stem cell properties in the adult hippocampus. Curr Opin Neurobiol. 2012; 22:754–61. [PubMed: 22503352]

Brecht M, Schneider M, Sakmann B, Margrie TW. Whisker movements evoked by stimulation of single pyramidal cells in rat motor cortex. Nature. 2004; 427:704–710. [PubMed: 14973477]

Cepeda C, Chen JY, Wu JY, Fisher RS, Vinters HV, Mathern GW, Levine MS. Pacemaker GABA synaptic activity may contribute to network synchronization in pediatric cortical dysplasia. Neurobiol Dis. 2014; 62:208–17. [PubMed: 24121115]

Chadwick EJ, Yang DP, Filbin MG, Mazzola E, Sun Y, Behar O, Pazyra-Murphy MF, Goumnerova L, Ligon KL, Stiles CD, Segal RA. A Brain Tumor/Organotypic Slice Co-culture System for Studying Tumor Microenvironment and Targeted Drug Therapies. J Vis Exp. 2015; 105:e53304.

Chen TW, Wardill TJ, Sun Y, Pulver SR, Renninger SL, Baohan A, Schreiter ER, Kerr RA, Orger MB, Jayaraman V, Looger LL, et al. Ultrasensitive fluorescent proteins for imaging neuronal activity. Nature. 2013; 499:295–300. [PubMed: 23868258]

Cohen I, Navarro V, Clemenceau S, Baulac M, Miles R. On the origin of interictal activity in human temporal lobe epilepsy in vitro. Science. 2002; 298:1418–21. [PubMed: 12434059]

Debanne D, Guérineau NC, Gähwiler BH, Thompson SM. Physiology and pharmacology of unitary synaptic connections between pairs of cells in areas CA3 and CA1 of rat hippocampal slice cultures. J Neurophysiol. 1995; 73:1282–1294. [PubMed: 7608771]

Duyckaerts C, Potier MC, Delatour B. Alzheimer disease models and human neuropathology: similarities and differences. Acta Neuropathol. 2008; 115:5–38. [PubMed: 18038275]

Emiliani V, Cohen AE, Deisseroth K, Häusser M. All-Optical Interrogation of Neural Circuits. J Neurosci. 2015; 35:13917–26. [PubMed: 26468193]

Eugène E, Cluzeaud F, Cifuentes-Diaz C, Fricker D, Le Duigou C, Clemenceau S, Baulac M, Poncer JC, Miles R. An organotypic brain slice preparation from adult patients with temporal lobe epilepsy. J Neurosci Methods. 2014; 235:234–244. [PubMed: 25064188]

Follenzi A, Santambrogio L, Annoni A. Immune responses to lentiviral vectors. Curr Gene Ther. 2007; 7:306–15. [PubMed: 17979677]

Gähwiler BH, Capogna M, Debanne D, McKinney RA, Thompson SM. Organotypic slice cultures: a technique has come of age. Trends Neurosci. 1997; 20:471–7. [PubMed: 9347615]

Hattiangady B, Shetty AK. Decreased neuronal differentiation of newly generated cells underlies reduced hippocampal neurogenesis in chronic temporal lobe epilepsy. Hippocampus. 2010; 20:97–112. [PubMed: 19309040]

Hioki H, Kameda H, Nakamura H, Okunomiya T, Ohira K, Nakamura K, Kuroda M, Furuta T, Kaneko T. Efficient gene transduction of neurons by lentivirus with enhanced neuron-specific promoters. Gene Ther. 2007; 14:872–82. [PubMed: 17361216]

Hocquemiller M, Giersch L, Audrain M, Parker S, Cartier N. Adeno-Associated Virus-Based Gene Therapy for CNS Diseases. Hum Gene Ther. 2016; 27:478–96. [PubMed: 27267688]

Hodge RD, Kowalczyk TD, Wolf SA, Encinas JM, Rippey C, Enikolopov G, Kempermann G, Hevner RF. Intermediate progenitors in adult hippocampal neurogenesis: Tbr2 expression and coordinate regulation of neuronal output. J Neurosci. 2008; 28:3707–17. [PubMed: 18385329]

Huberfeld G, Wittner L, Clemenceau S, Baulac M, Kaila K, Miles R, Rivera C. Perturbed Cl- homeostasis and GABAergic signaling in human temporal lobe epilepsy. J Neurosci. 2007; 27:9866–73. [PubMed: 17855601]

Jones RS, da Silva AB, Whittaker RG, Woodhall GL, Cunningham MO. Human brain slices for epilepsy research: Pitfalls, solutions and future challenges. J Neurosci Methods. 2016; 260:221–32. [PubMed: 26434706]

Koh JY, Choi DW. Quantitative determination of glutamate mediated cortical neuronal injury in cell culture by lactate dehydrogenase efflux assay. J Neurosci Methods. 1987; 20:83–90. [PubMed: 2884353]

Köhling R, Lücke A, Straub H, Speckmann EJ, Tuxhorn I, Wolf P, Pannek H, Oppel F. Spontaneous sharp waves in human neocortical slices excised from epileptic patients. Brain. 1998; 121:1073–87. [PubMed: 9648543]

Kwan AC, Dan Y. Dissection of cortical microcircuits by single-neuron stimulation in vivo. Curr Biol. 2012; 22:1459–67. [PubMed: 22748320]

Le Duigou C, Simonnet J, Telenczuk MT, Fricker D, Miles R. Recurrent synapses and circuits in the CA3 region of the hippocampus: an associative network. Front Cell Neurosci. 2014; 7:262. [PubMed: 24409118]

Lentz TB, Gray SJ, Samulski RJ. Viral vectors for gene delivery to the central nervous system. Neurobiol Dis. 2012; 48:179–88. [PubMed: 22001604]

Li CY, Poo MM, Dan Y. Burst spiking of a single cortical neuron modifies global brain state. Science. 2009; 324:643–646. [PubMed: 19407203]

Lillis KP, Wang Z, Mail M, Zhao GQ, Berdichevsky Y, Bacskai B, Staley KJ. Evolution of network synchronization during early epileptogenesis parallels synaptic circuit changes. J Neurosci. 2015; 35:9920–34. [PubMed: 26156993]

Long C, Fureman B, Dingledine R. 2014 Epilepsy Benchmarks: Progress and Opportunities. Epilepsy Curr. 2016; 16:179–81. [PubMed: 27330449]

Maglóczky Z, Halász P, Vajda J, Czirják S, Freund TF. Loss of Calbindin-D28K immunoreactivity from dentate granule cells in human temporal lobe epilepsy. Neuroscience. 1997; 76:377–85. [PubMed: 9015323]

Mahoney C, Feliciano DM, Bordey A, Hartman NW. Switching on mTORC1 induces neurogenesis but not proliferation in neural stem cells of young mice. Neurosci Lett. 2016; 614:112–8. [PubMed: 26812181]

Marco P, Sola RG, Pulido P, Alijarde MT, Sánchez A, Ramón y Cajal S, DeFelipe J. Inhibitory neurons in the human epileptogenic temporal neocortex: an immunocytochemical study. Brain. 1996; 119:1327–47. [PubMed: 8813295]

McBain CJ, Boden P, Hill RG. Rat hippocampal slices in vitro display spontaneous epileptiform activity following long-term organotypic culture. J Neurosci Methods. 1989; 27:35–49. [PubMed: 2563782]

Mioduszewska B, Jaworski J, Szklarczyk AW, Klejman A, Kaczmarek L. Inducible cAMP early repressor (ICER)-evoked delayed neuronal death in the organotypic hippocampal culture. J Neurosci Res. 2008; 86:61–70. [PubMed: 17722060]

Nicholls JG, Purves D. Monosynaptic chemical and electrical connexions between sensory and motor cells in the central nervous system of the leech. J Physiol. 1970; 209:647–667. [PubMed: 5499801]

Ozbas-Gerçeker F, Redeker S, Boer K, Ozgüç M, Saygi S, Dalkara T, Soylemezoglu F, Akalan N, Baayen JC, Gorter JA, Aronica E. Serial analysis of gene expression in the hippocampus of patients with mesial temporal lobe epilepsy. Neuroscience. 2006; 138:457–74. [PubMed: 16413123]

Paliouras GN, Hamilton LK, Aumont A, Joppé SE, Barnabé-Heider F, Fernandes K. Mammalian target of rapamycin signaling is a key regulator of the transit-amplifying progenitor pool in the adult and aging forebrain. J Neurosci. 2012; 32:15012–26. [PubMed: 23100423]

Pallud J, Le Van Quyen M, Bielle F, Pellegrino C, Varlet P, Labussiere M, Cresto N, Dieme MJ, Baulac M, Duyckaerts C, Kourdougli N, et al. Cortical GABAergic excitation contributes to epileptic activities around human glioma. Sci Transl Med. 2014; 6:244ra89.

Paquet D, Kwart D, Chen A, Sproul A, Jacob S, Teo S, Olsen KM, Gregg A, Noggle S, Tessier-Lavigne M. Efficient introduction of specific homozygous and heterozygous mutations using CRISPR/Cas9. Nature. 2016; 533:125–9. [PubMed: 27120160]

Pernhorst K, Herms S, Hoffmann P, Cichon S, Schulz H, Sander T, Schoch S, Becker AJ, Grote A. TLR4, ATF-3 and IL8 inflammation mediator expression correlates with seizure frequency in human epileptic brain tissue. Seizure. 2013; 22:675–8. [PubMed: 23706953]

Pineda JR, Encinas JM. The contradictory effects of neuronal hyperexcitation on adult hippocampal neurogenesis. Front Neurosci. 2016; 10:74. [PubMed: 26973452]

Prida LM, Huberfeld G, Cohen I, Miles R. Threshold behavior in the initiation of hippocampal population bursts. Neuron. 2006; 49:131–42. [PubMed: 16387645]

Schwartzkroin PA, Knowles WD. Intracellular study of human epileptic cortex: in vitro maintenance of epileptiform activity? Science. 1984; 223:709–12. [PubMed: 6695179]

Seifert S, Sontheimer H. Bradykinin enhances invasion of malignant glioma into the brain parenchyma by inducing cells to undergo amoeboid migration. J Physiol. 2014; 592:5109–27. [PubMed: 25194042]

Selke K, Müller A, Kukley M, Schramm J, Dietrich D. Firing pattern and calbindin-D28k content of human epileptic granule cells. Brain Research. 2006; 1120:191–201. [PubMed: 16997289]

Stoppini L, Buchs PA, Muller D. A simple method for organotypic cultures of nervous tissue. J Neurosci Methods. 1991; 37:173–82. [PubMed: 1715499]

Trevelyan AJ, Sussillo D, Watson BO, Yuste R. Modular propagation of epileptiform activity: evidence for an inhibitory veto in neocortex. J Neurosci. 2006; 26:12447–55. [PubMed: 17135406]

Tye KM, Prakash R, Kim SY, Fenno LE, Grosenick L, Zarabi H, Thompson KR, Gradinaru V, Ramakrishnan C, Deisseroth K. Amygdala circuitry mediating reversible and bidirectional control of anxiety. Nature. 2011; 471:358–62. [PubMed: 21389985]

van Hooijdonk LW, Ichwan M, Dijkmans TF, Schouten TG, de Backer MW, Adan RA, Verbeek FJ, Vreugdenhil E, Fitzsimons CP. Lentivirus-mediated transgene delivery to the hippocampus reveals sub-field specific differences in expression. BMC Neurosci. 2009; 10:2. [PubMed: 19144149]

Vargas-Caballero M, Willaime-Morawek S, Gomez-Nicola D, Perry VH, Bulters D, Mudher A. The use of human neurons for novel drug discovery in dementia research. Expert Opin Drug Discov. 2016; 11:355–67. [PubMed: 26878555]

Venkatesh HS, Johung TB, Caretti V, Noll A, Tang Y, Nagaraja S, Gibson EM, Mount CW, Polepalli J, Mitra SS, Woo PJ, et al. Neuronal Activity Promotes Glioma Growth through Neuroligin-3 Secretion. Cell. 2015; 161:803–16. [PubMed: 25913192]

Wittner L, Huberfeld G, Clémenceau S, Eross L, Dezamis E, Entz L, Ulbert I, Baulac M, Freund TF, Maglóczky Z, Miles R. The epileptic human hippocampal cornu ammonis 2 region generates spontaneous interictal-like activity in vitro. Brain. 2009; 132:3032–46. [PubMed: 19767413]

Zhou X, Clister TL, Lowry PR, Seldin MM, Wong GW, Zhang J. Dynamic visualization of mTORC1 activity in living cells. Cell Rep. 2015; 10:1767–1777.

Europe PMC Funders Author Manuscripts

Europe PMC Funders Author Manuscripts

Highlights

- Organotypic culture of brain tissue from neurological patients aged 3-62 years.
- Optimized transduction of transgenes carried by viral vectors.
- Imaging of multi-cellular activity (GCaMP) and intra-cellular signaling (mTOR).
- Imaging window from 12 days, for transgene expression, until~50 days in culture.

Europe PMC Funders Author Manuscripts

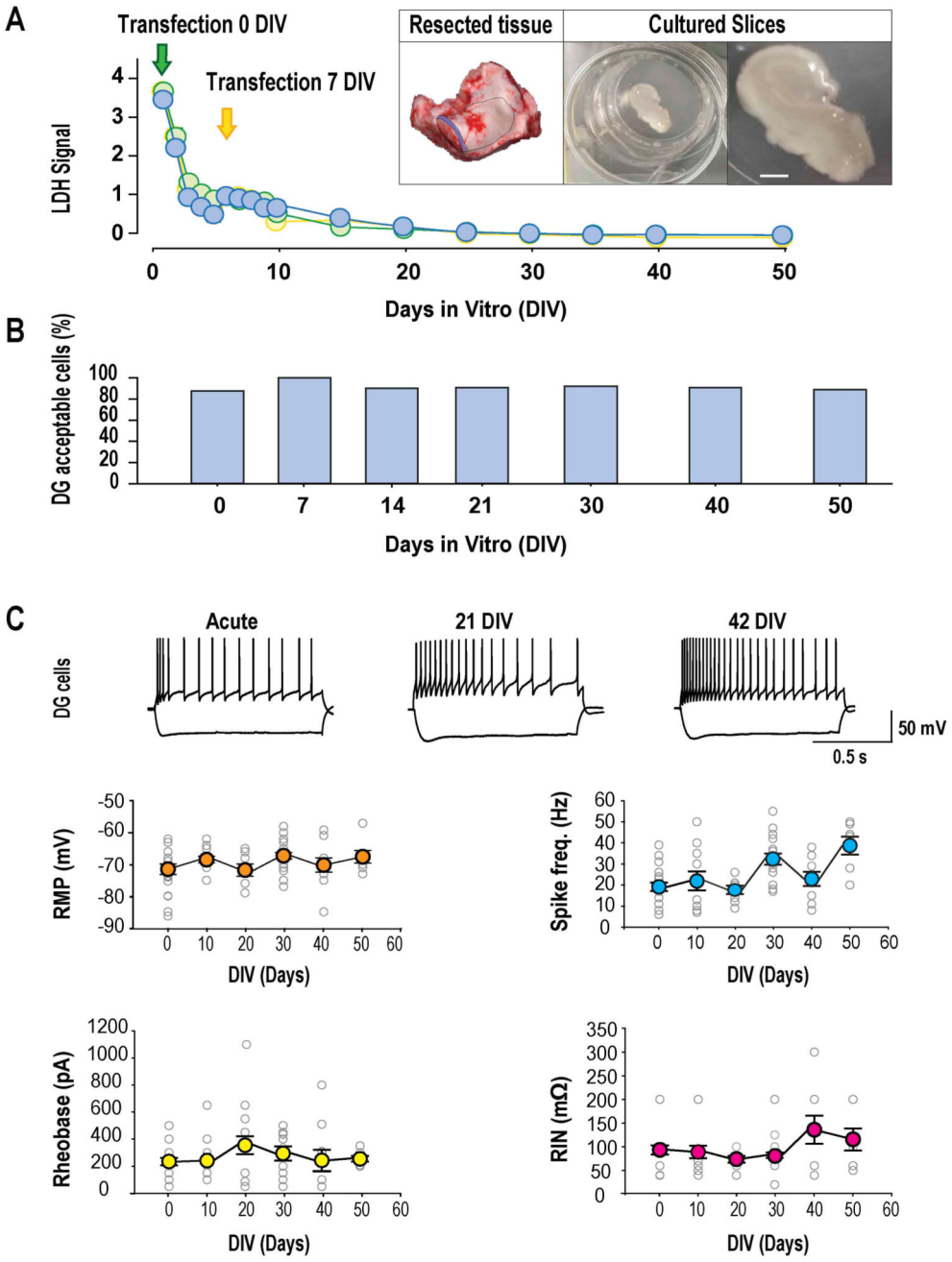

Figure 1. Stability of organotypic cultures with time in culture.

(A) Changes in lactate dehydrogenase (LDH) levels in supernatant of sclerotic temporal lobe cultures with days in vitro (DIV). LDH signals were high from 1-4 DIV and then declined. They increased transiently when antibiotics were withdrawn at 7 DIV but viral vector application had no effect (blue, no application; green, application at 0 DIV; orange at 6 DIV). Inset shows a temporal lobe tissue block, a slice in culture and a slice ready for recording, left to right. **(B)** Variation with time of acceptable (RMP < -55 mV, multi-spike response to current stimulation) / attempted whole-cell records from dentate granule cells.

Acceptable records were obtained from 94% of dentate granule cell, 74% of CA2/3 pyramidal cells, 40 % of subicular pyramidal cells 40% and 44% of cortical pyramidal cells. **(C)** Changes in dentate granule cell electrophysiology with DIV. Insets above show effects of depolarizing and hyperpolarizing current injections (1 sec duration) at 0 (Acute), 21 and 42 DIV. Below graphs of variation with time for resting membrane potential (RMP), firing frequency (Spike freq), rheobase and input resistance (R_{in}). Data for each time point from 10-35 neurons.

Europe PMC Funders Author Manuscripts

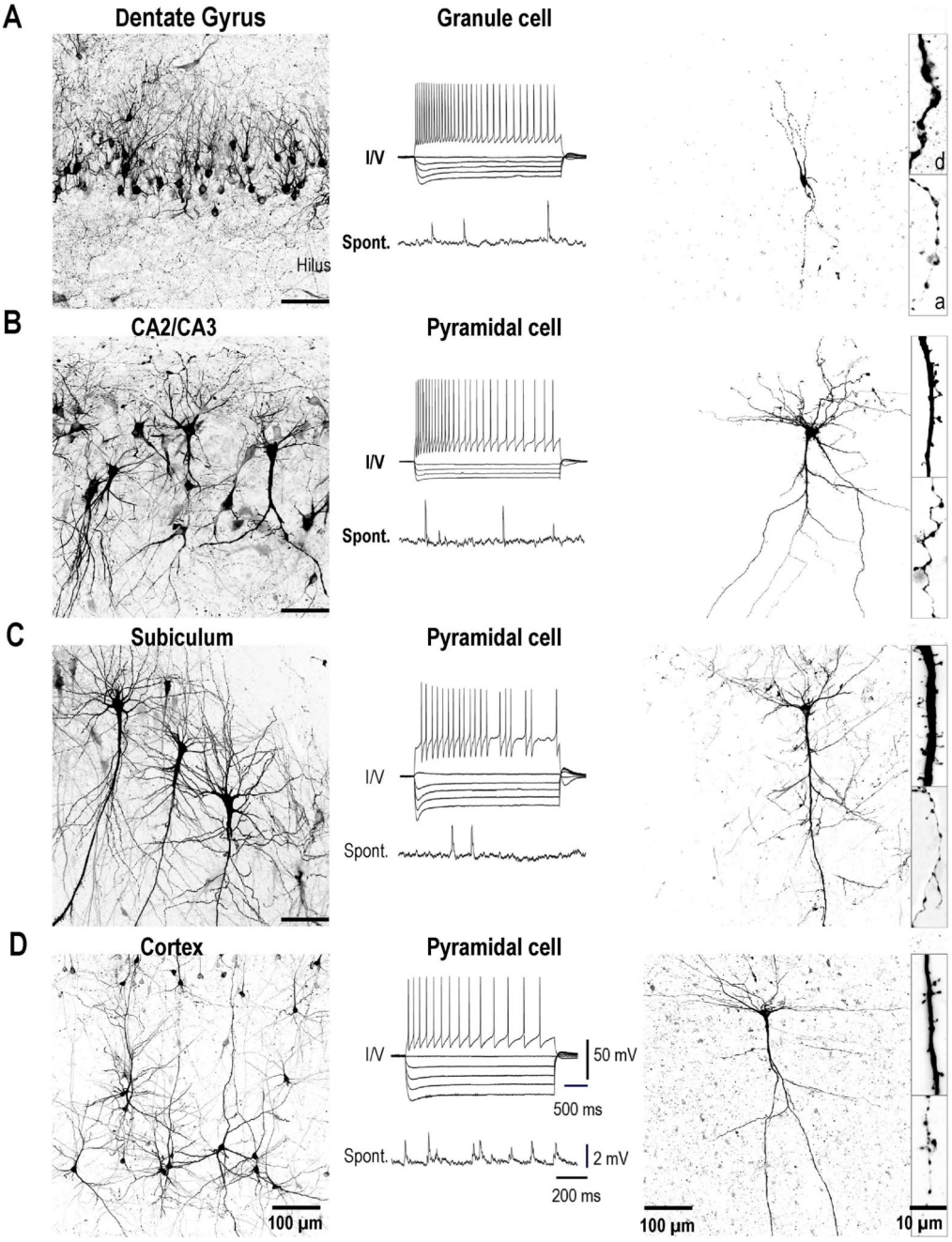

Figure 2. Regional differences in neuronal organization, firing and form after 14-40 DIV.

Neuronal organization, physiology and anatomy for **(A)** Dentate gyrus, **(B)** CA2/3 region and **(C)** subiculum of sclerotic temporal lobe and **(D)** layers II-III of dysplasic cortex at 20-40 DIV. Left: neuronal organization revealed as Golgi-like images from immuno-staining against GFP from cultures with GCaMP-transduced neurons. Middle: whole cell records of principal cells with current induced firing and hyperpolarization (pulse duration 1 sec, amplitude ± 300 pA) and spontaneous synaptic events, below. Right: soma and proximal dendrites of biocytin-filled neurons. Insets show dendritic and axonal sections.

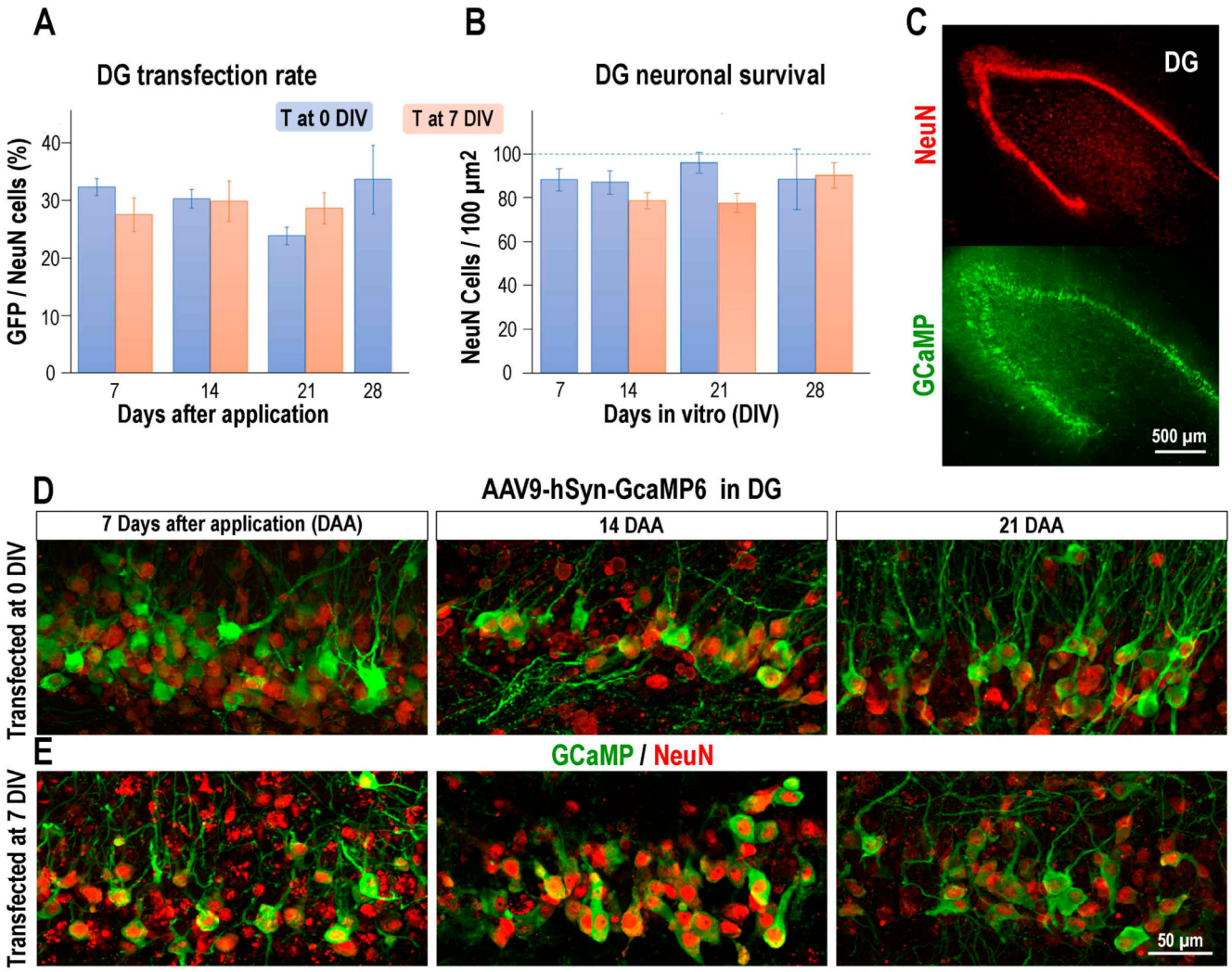

Figure 3. Viral vector transduction in organotypic culture.

(A) Transduction rate, T, as GFP^+ cells / $NeuN^+$ cells, and **(B)** survival, density of $NeuN^+$ cells at each DIV / density in acute (0DIV) tissue, for dentate granule cells. Data from delays of 7-28 days after applying the AAV9.hSyn.GCaMP6f vector during culture preparation (0 DIV, blue) or at 1 week in culture (7 DIV, orange). **(C)** The dentate gyrus, immuno-stained for NeuN (red, upper) and GFP (for GCaMP, green, lower), at 14 DIV after vector application at 0 DIV. **(D)** Dentate granule cells stained for NeuN (red) and GFP (green) at 7, 14 and 21 days after vector application at 0DIV. **(E)** As (d) but with vector application at 7DIV.

Europe PMC Funders Author Manuscripts

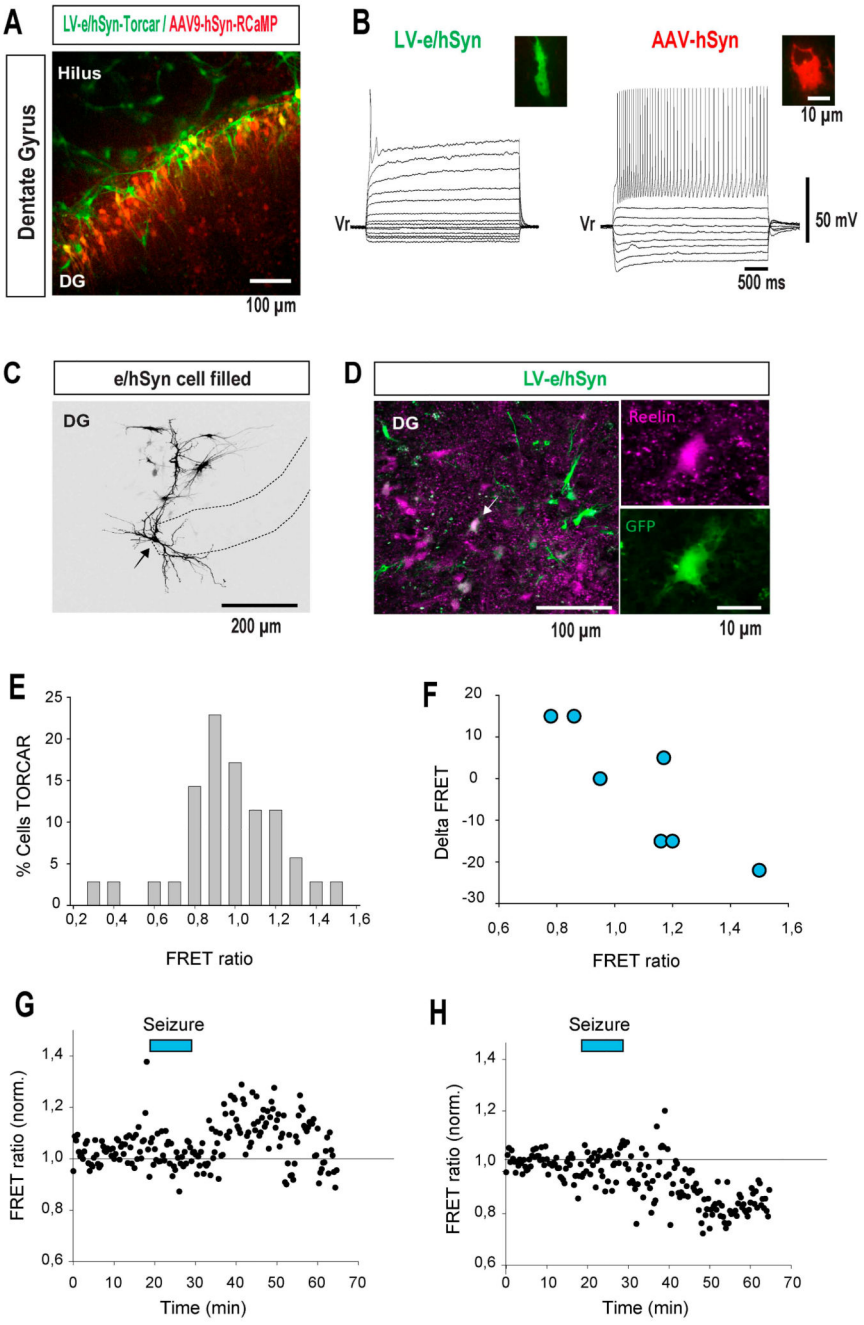

Figure 4. Viral vector transduction: cell types, mTORC1 activity.

(A) Dual transfection with the vectors AAV9.hSyn.RCaMP6 (red) and LV-e/hSyn-Torcar-GFP (green). Fluorescence in the dentate region at 14 days after vector application at 0DIV. **(B)** Typical responses to depolarizing and hyperpolarizing current injected into cells transduced with LV-e/hSyn-Torcar-GFP (left) and AAV9.hSyn.RCaMP6 (right). **(C)** Multiple cells recovered after biocytin injection into one recorded cell transduced with the LV-e/hSyn-Torcar-GFP vector. **(D)** Immunostaining for reelin Scale bar 100 µm, 10 µm. **(E)** Distribution of Fret ratios reflecting mTORC1 kinase activity from cells transduced with LV-

e/hSyn-Torcar-GFP in basal conditions (n=xx neurons from xx slice cultures). **(F)** Changes in mTORC1 kinase activity derived from FRET ratio, induced by seizure activity plotted against basal kinase activity (n=7 neurons from xx slice cultures). Effects of seizure activity on **(G)** one neuron with a low initial mTORC1 kinase activity and **(H)** another neuron with a high initial activity. The ratio FRET is normalized.

Europe PMC Funders Author Manuscripts

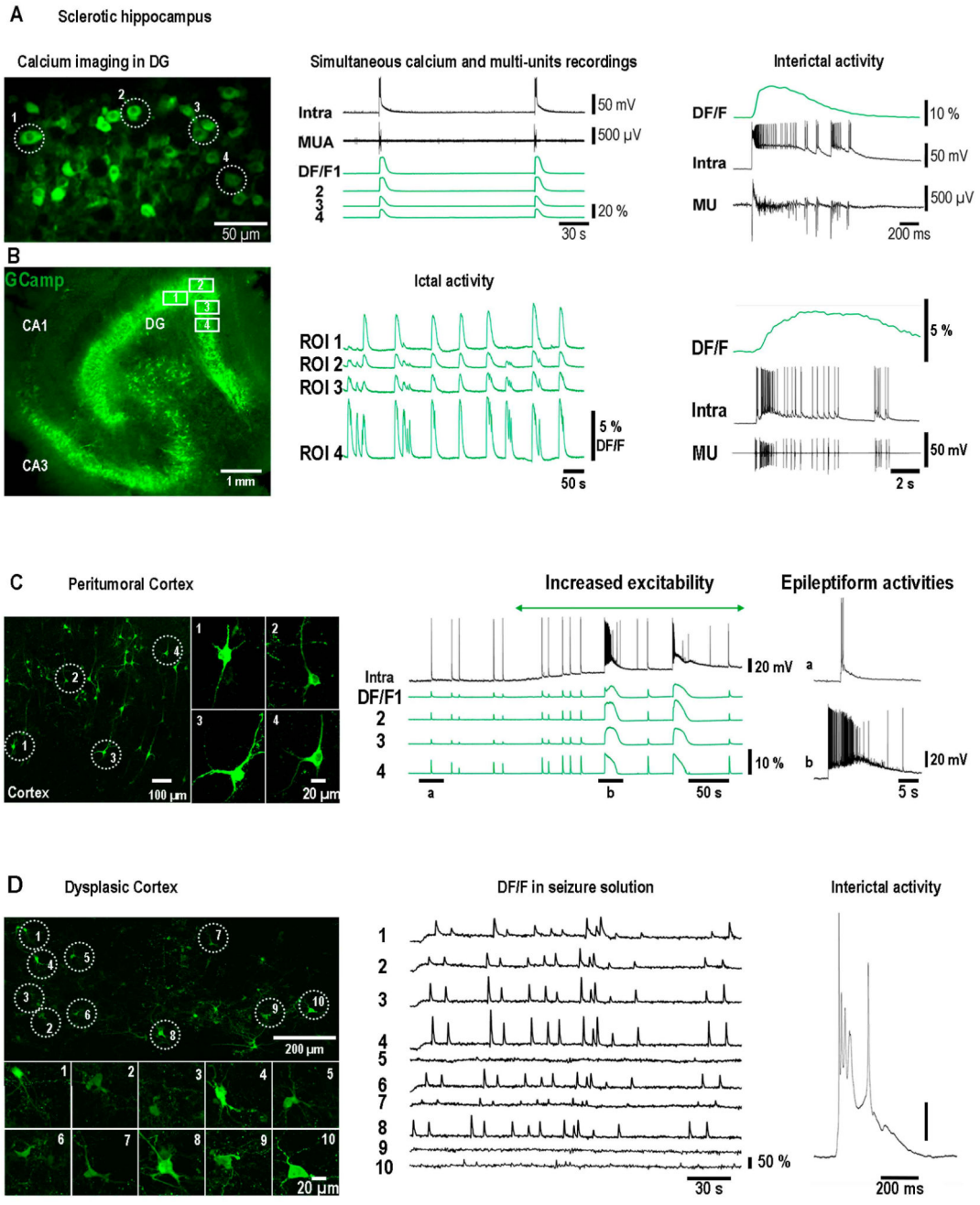

Figure 5. Calcium imaging of epileptiform activities in organotypic culture.

(A) Epileptiform activity generated in the dentate region of a medial temporal lobe culture at 22DIV. Intracellular record, local field potential with multi-unit activity (MUA) and Ca-transients (DF/F) for four granule cells, 1-4, transduced with GCaMP6. All traces are shown for a single interictal event in detail at right. **(B)** Induced ictal-like synchrony (K^+, 10; Mg^{++}, 0.1 mM). Snapshot of GCaMP signals from the dentate, hilus and CA2/3 regions during an ictal event. Time course of intracellular Ca^{++} signals (DF/F) from 4 sites (1-4, white squares) in the dentate cell body layer. Right: ictal-like event recorded as Ca-transient

Europe PMC Funders Author Manuscripts

(DF/F), single cell (Intra) and local field potential (MUA) **(C)** Epileptiform activities generated by an organotypic culture of peritumoral cortex (xxDIV). GCaMP signals obtained from identified cortical neurons 1-4 (left) are shown with a whole cell record from another pyramidal cell during the transition from control to a high-excitability external solution (K^+, 10; Mg^{++}, 0.1 mM). Ca transients increase in duration and amplitude from time a to time b as the intensity and duration of pyramidal cell burst firing increases. **(D)** Epileptiform activities generated by a culture of peri-tumoral cortex (xxDIV). GCaMP signals (DF/F) from pyramidal cells 1-10 (left) during exposure to a high-excitability external solution (K^+, 10; Mg^{++}, 0.1 mM). Synchronous Ca- transients were generated by cells 1, 2, 3, 4, 6 and 8 but were small or absent in cells 5, 7, 9 and 10. Whole cell record at right shows a representative intracellular epileptiform burst.

Europe PMC Funders Author Manuscripts

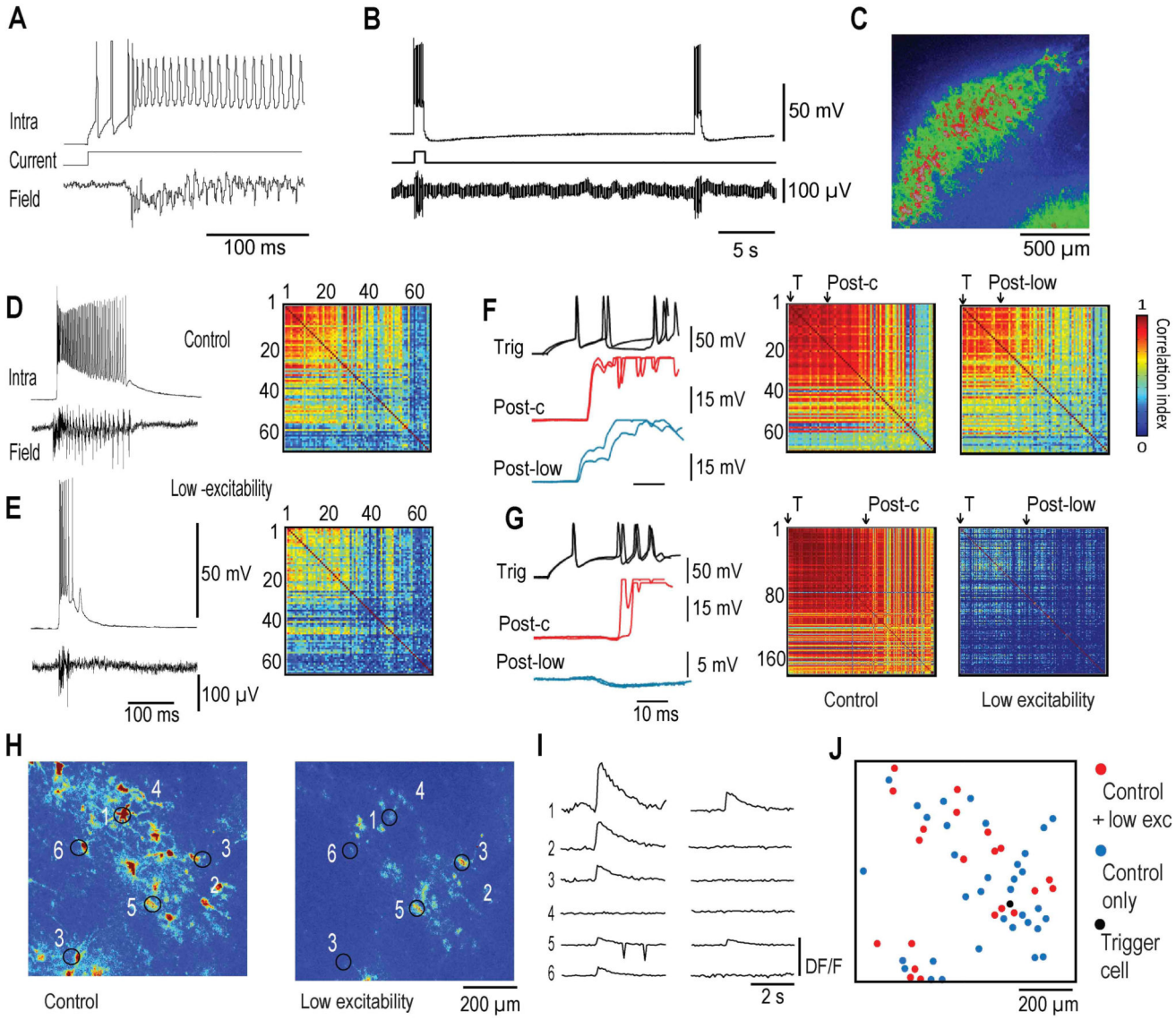

Figure 6. Synaptic circuits for epileptic synchrony in culture.

(A) Stimulation of a single CA2/3 pyramidal cell initiated a local epileptiform field potential. Sclerotic hippocampal culture at 18 DIV. **(B)** Events triggered by a single cell (trig) were comparable in field potential amplitude and duration to spontaneously occurring (spont) epileptiform events. **(C)** Single cell stimulation induced a Ca-transient (DF/F) in many local GCaMP-transfected neurons. **(D, E)** Reducing neuronal excitability resulted in shorter duration field potentials with fewer neurons participating in spontaneous epileptiform Ca-transients. This change is reflected in a reduced number of cells with synchronous Ca-transients in matrix plots, to the right. **(F)** Paired record from a trigger cell and a follower neuron. The transition from control (red trace) to low excitability (blue trace) reduced firing and revealed a mono-synaptic EPSP. Matrix plots fromcontrol and low excitability conditions shown at right. The trigger cell (1 in the matrix order) and recorded follower cell, with a Ca-transient in low excitability, indicated by arrows. **(G)** Paired record

from a trigger cell and a follower neuron where the transition from control (red trace) to low excitability+ (blue trace) revealed a poly-synaptic IPSP. Matrix plots at right. Trigger cell (1 in the matrix order) and recorded follower cell, with no Ca-transient in low excitability, indicated by arrows. **(H)** Averages of GCaMP signals from a field of ~600x600 μm^2 in the CA2/3 region (n=8 epileptiform events) after firing in a trigger cell in control and low excitability conditions. **(H)** Signals from selected cells of **(H)** before and after switching from control to low-excitability. **(J)** Connectivity map corresponding to cells in **(H)** showing the triggering cell (black) cells that generated a Ca-transient only in the control solution (blue) and neurons showing a Ca-transient in both control and low excitability conditions.

Europe PMC Funders Author Manuscripts